

HELICOPTER OPERATIONS TO MOVING OFFSHORE HELIDECKS

A PRACTICAL ANALYTICAL MODEL OF THE STABILITY RESERVE OF A HELICOPTER ON A MOVING HELIDECK

Athena Scaperdas, athena.scaperdas@atkinglobal.com, Atkins Oil & Gas (UK)
Dave Howson, dave.howson@caa.co.uk, Civil Aviation Authority (UK)

Abstract

The Oil and Gas industry relies heavily on helicopters for transporting personnel and cargo to offshore installations and support vessels. A growing number of offshore helicopter operations are to moving helidecks on large vessels such as FPSOs, drillships, semi-submersibles, as well as smaller service vessels.

Landing on a moving helideck presents additional challenges, not only at the point of touchdown but also during the entire duration the helicopter remains on the helideck. Once on deck, the helicopter wheels are braked and there is usually a net on the helideck to resist sliding, but the helicopter is not secured onto the helideck in any other way. During a typical 20minute-long landing turn-around, the helicopter rotors are kept running. Although the main rotor collective pitch is set at its minimum value (MPOG), a significant amount of lift can be generated, which increases with wind speed. Combined with the destabilising effect of the helideck motion and side wind drag, this can cause the helicopter to roll over or slide.

As discussed in more detail in [1], Atkins has carried out research on behalf of the UK Civil Aviation Authority to improve the operational criteria used to decide when it is safe to land on moving offshore helidecks. A central element of this research has been to develop a practical analytical model of the reserve of stability of a helicopter on a moving helideck.

A complete analytical model of helicopter stability has been successfully developed that covers all modes of on-deck failure (roll-over and sliding), for a nose wheel tricycle undercarriage helicopter. The associated analytical expressions that have been derived are remarkably simple, physically intuitive, and make the relative contribution of all the destabilising factors easy to understand and assess. These analytical expressions can be used to calculate the reserve of stability of any helicopter in real time, as well as for calculating operational limits. This approach has many advantages compared to 'black box' modelling methods.

One of the most important unknowns has been the main rotor lift at MPOG. An empirical model of the lift has been developed, based on experimental and field data. Other modelling aspects that present difficulties or rely on obtaining proprietary data are also discussed, including how to obtain a general, simple correlation for fuselage wind drag, and measuring the vertical position of the centre of gravity of a helicopter.

Finally, a comparison and evaluation of the model against results from dedicated field trials is presented, together with a discussion and recommendations for further work.

1. INTRODUCTION

The Oil and Gas industry relies heavily on helicopters for transporting personnel and cargo to offshore installations and support vessels. A growing number of offshore helicopter operations are to moving helidecks on large vessels such as FPSOs, drillships, semi-submersibles, as well as smaller service vessels.

Landing on a moving helideck presents additional challenges, not only at the point of touchdown but also during the entire duration the helicopter remains on the helideck. Once on deck, the helicopter wheels are braked and there is usually a net on the helideck to resist sliding, but the helicopter is not

secured onto the helideck in any other way. During a typical 20minute-long landing turn-around, the helicopter rotors are kept running. Although the main rotor collective pitch is set at its minimum value (MPOG), a significant amount of lift can be generated which increases with wind speed. Combined with the destabilising effect of the helideck motion and side wind drag, this can cause the helicopter to roll over or slide.

As discussed in more detail in [1], Atkins has carried out research on behalf of the UK Civil Aviation Authority to improve the operational criteria used to decide when it is safe to land on moving offshore helidecks. A central element of this research has been to develop a practical analytical model of the

reserve of stability of a helicopter on a moving helideck.

What was required was a model that would:

- be as transparent as possible, accessible to all stakeholders;
- clarify the relative contribution of all the destabilising factors;
- identify the most important input parameters;
- identify which helideck motion and wind parameters best correlate with a helicopter's reserve of stability and therefore help decide which critical parameters should be used to predict helicopter on-deck safety prior to landing;
- be customisable to cover all the different helicopter types operating in the North Sea and to cover all realistic operational scenarios;
- be fast to run, allowing the whole range of real-life operational scenarios to be assessed, e.g. as part of a probabilistic risk calculation;
- set out all assumptions clearly;
- be backed by experimental evidence and best available data;
- allow independent checking and lend itself to continuous improvement.

It is possible in principle to assess whether a helicopter will tip over or slide, by calculating all the forces and moments acting on the helicopter and then using the equilibrium equations in six degrees of freedom. Each of the forces/moments acting on the helicopter can be calculated by a separate sub-model, and then all forces and moments can be input to the equilibrium equations for each of the modes of failure to determine if the point of failure has been reached. Such a model should, in theory, be relatively straightforward for a helicopter original equipment manufacturer (OEM) or technical consultancy to build, using existing simulation models and integrating them with software such as FlightLab.

Nonetheless, any such calculation would still require a large number of inputs and assumptions (at least 6 parameters for helideck motion alone), and such a model also would have to be adapted in some way to calculate limits of operability based on a few salient parameters.

Currently, the maximum roll, pitch, inclination and heave/heave rate of the helideck are the only criteria used to assess the destabilising effect of helideck motion. However, it is evident that helideck accelerations in all three directions also contribute to destabilising a helicopter. It is impractical, however, to use so many different parameters to describe the effect of helideck motion to pilots. Instead, the CAA stipulated that the destabilising effect of the helideck should ideally be expressed in terms of a single measure. This has been achieved and the single

measure is the Measure of helideck Motion Severity (MMS).

Over the course of the research it has become clear that the wind is also an important destabilising factor, and that a further parameter to describe the severity of the wind conditions (Wind Severity Index) would have to be defined.

In response to this very challenging research remit, a complete analytical model of helicopter stability has been successfully developed that fulfils all the above objectives. It covers all modes of on-deck failure (roll-over and sliding), for a nose wheel tricycle undercarriage helicopter.

2. MODELLING ON-DECK STABILITY

2.1 Modelling the forces acting on the helicopter while on-deck

A number of forces act on a helicopter on a moving helideck:

- helicopter weight (i.e. gravitational force);
- inertial forces acting on the helicopter due to helideck acceleration;
- fuselage wind drag forces;
- main rotor lift;
- main rotor torque;
- control forces - main rotor cyclic forces and tail rotor force.

2.2 Gravitational and inertial forces, F_G

The helicopter weight and the inertial forces due to the acceleration of the moving helideck can be combined into one force, F_G , directly proportional to the total gravitational and inertial acceleration, a , equal to:

$$(1) \quad \vec{F}_G = m \cdot \vec{a}$$

It acts at the centre of gravity (CoG), which is assumed to be located at a distance CGX away from the nose wheel, displaced laterally from the longitudinal axis of the helicopter by CGY, and a distance CGZ above the ground.

Provided that the mass of the helicopter and the position of the CoG is known accurately, F_G can be measured on a moving helideck fitted with MRUs (Motion Reference Units) with a very high degree of accuracy.

2.3 Fuselage wind drag

The fuselage wind drag F_w , is expected to be proportional to the square of the wind, i.e. it can be expressed in the form:

$$(2) \quad F_w(U, \beta) = k_w(\beta) \cdot U^2$$

where β is the wind direction relative to the longitudinal axis of the helicopter, and k_w is a constant of proportionality equal to:

$$(3) \quad k_w(\beta) = \frac{1}{2} \cdot \rho \cdot A(\beta) \cdot C_d(\beta)$$

which in turn depends on ρ , the air density, C_d , the drag coefficient, and A the cross-sectional area of the fuselage presented to a given relative wind direction β .

The wind drag acts at the Centre of Pressure, in the direction of the wind. It can also be referred at any other point, by including additional moments as appropriate.

Drag coefficients are typically measured in the wind tunnel with scaled models or modelled using CFD (Computational Fluid Dynamics). Such information is typically kept confidential by helicopter OEMs, and is not published in the open literature.

Confidential fuselage drag data for two helicopter types were made available for use in this project. However, in order to derive generic operational limits, the drag of all other in-service helicopter types needs to be evaluated. The possibility of deriving a simple parametric representation to estimate the drag coefficient for any type of helicopter based on a few key dimensions was investigated as follows.

The constant of proportionality k_w depends on both A and C_d , and both are a function of wind direction β . Nonetheless, helicopter shapes are generally similar, being long ellipsoids with a tail boom and fin attached at the back. It was considered therefore that the fuselage side area, A_{side} , could be used as the basis for a rough estimate of the drag of helicopters of different sizes.

By plotting the drag coefficients for two helicopter types (as provided by helicopter OEMs) in the form of the ratio, R_w :

$$(4) \quad R_w(\beta) = \frac{A(\beta) \cdot C_d(\beta)}{A_{side}}$$

the data from the two helicopters collapsed onto very similar curves, as shown in Figure 1.

The maximum value of R_w occurs at $\beta=90\text{deg}$ (i.e. for a beam wind), and is equal to C_d (since $A_{side}=A(90\text{deg})$). The data in Figure 1 suggest a beam-on C_d value that is roughly of the order of 1.

The minimum value of R_w corresponds to $\beta=0\text{deg}$. It is equal to C_d times the ratio of the frontal and side

areas, A_{front}/A_{side} . The ratio of A_{front}/A_{side} is of the order of 0.2 and likely to be similar for different helicopter types. $C_d(0\text{deg})$ is expected to be broadly of the order of 0.2 (e.g. based on published data in [2]) and, as a result, $R_w(0\text{deg})$ is a small number close to zero.

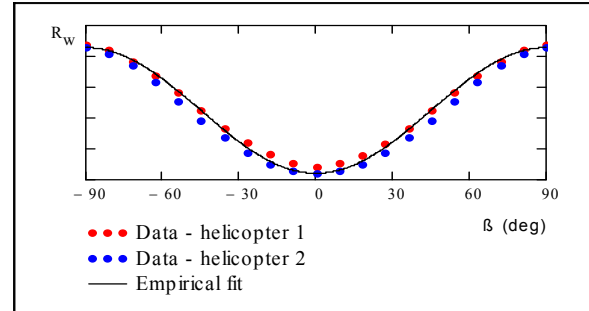


Figure 1 A comparison of R_w for two helicopter types.

A sinusoidal curve can be used to fit between the values at 0 and 90deg, as follows:

$$(5) \quad R_w(\beta) = \frac{(\max + \min)}{2} - \frac{(\max - \min)}{2} \cdot \cos(2\beta)$$

where:

$$\max = R_w(90\text{deg}), \approx 1$$

$$\min = R_w(0\text{deg}), \approx 0$$

Using values for max and min corresponding to available data for the two helicopter types, provides a reasonably good fit for the variation of R_w as a function of β (as shown in Figure 1).

Clearly, it would be desirable to test this empirical fit against accurate C_d data for a wider range of helicopter types. A method for estimating the position of the centre of pressure is also currently being developed.

2.4 Main rotor lift force modelling

When the helicopter is on-deck, the collective pitch is set at its minimum value (MPOG) and the cyclic is set at its central setting. However, even at this 'idle' setting, a significant lift force can be generated.

Although rotor models exist that can predict the rotor lift as a function of blade collective pitch and other rotor parameters (whether blade integral models or CFD models), information from such models has proven unreliable, with some models predicting negative values of lift at MPOG. For this reason, it was judged that the only reliable way forward was to measure the lift at MPOG directly, during field trials.

The first set of trials was carried out by landing a Sikorsky S-76 on the helideck of the Foinaven

FPSO, as discussed in more detail later in Section 7.1. This provided proof for the first time that the main rotor lift at MPOG:

- is positive (i.e. directed upwards);
- increases with wind speed (for the S-76, about 1,000kgf at 10m/s and about half that in zero wind);
- is a significant fraction of helicopter weight, and therefore an important destabilising factor.

It was also expected that the angle of attack of the rotor relative to the wind, α_s , should also influence the lift. Because the rotor mast is typically inclined forward by an angle γ , then α_s should in turn be a function of γ , relative wind direction β and helideck angle relative to the wind. Any local updrafts/downdrafts on the helideck (induced by the superstructure of the vessel) would also affect α_s .

In order to derive more data for the lift at MPOG, another set of trials was performed, this time involving a Super Puma AS332-L2 helicopter at Aberdeen airport. Two sets of tests were carried out: a) in zero wind, and b) in a wind of about 10m/s. To test the dependence of the lift on angle of attack α_s , the orientation of the helicopter relative to the wind was varied to make use of the built-in main rotor mast tilt, γ . The α_s settings ranged from about -5deg ($\alpha_s=\gamma$, for a head-on wind direction), to +5deg ($\alpha_s=-\gamma$ for a tail-on direction). It was found that, for the Super Puma, the lift also varied significantly with wind speed; the lift at 10m/s was about 1,000kgf, nearly double that at zero wind. The lift also varied significantly with α_s (data points from the Aberdeen trials are included as circles in Figure 3, as discussed later).

The lift generated by both the S-76 and the Super Puma at zero wind and at wind speeds of about 10m/s, were very similar. This was an unexpected result, since the Super Puma is a much heavier helicopter with a larger rotor, and was thus expected to generate more lift than the S-76 at MPOG in the same wind conditions.

In order to understand this behaviour more fully, and to gain insight into the lift generated at wind speeds higher than 10m/s, the option of further trials was considered. Organising field trials in high winds had already proved very difficult (since they occur relatively rarely and unpredictably), and scaled rotor models in the wind tunnel are not considered reliable enough.

However, it is possible to carry out full-scale helicopter tests. The NASA Ames 80x120 ft wind tunnel, is the largest wind tunnel in the world, and is large enough to accommodate a full-sized helicopter. The option of carrying out such trials for this project was considered, and this line of enquiry led to the discovery of detailed full-scale S-76

measurements from a previous, unrelated trial carried out by NASA Ames. This comprehensive dataset [3] contains raw measurements of lift and other main rotor forces as a function of collective pitch (from 2 to 4deg upwards), wind speed (from 0 to 50m/s) and angle of attack (from -10 to +10deg). The following patterns emerged from a meta-analysis of this data:

- for any given set of U and α_s values, the lift increased linearly with collective pitch, θ . This applied consistently to all measurements (as shown in Figure 2, using $\alpha_s=-2$ deg as an example);
- the lift increased with wind speed, and the way in which the lift increased depended on α_s .

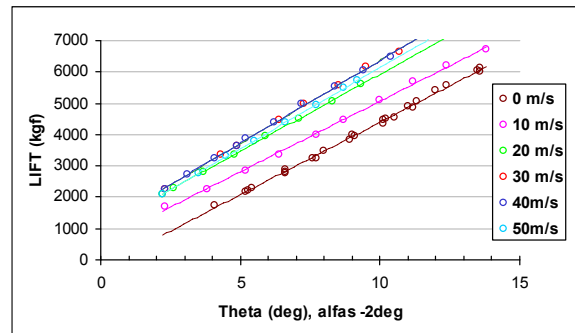


Figure 2: The linear variation of main rotor lift as a function of collective pitch θ , for any given combination of wind speed U and angle of attack, α_s (range of wind speeds, $\alpha_s=-2$ deg shown as an example).

Although the NASA Ames measurements were performed for constant increments of wind speed and α_s , the values of θ chosen were arbitrary. Exploiting the fact that lift depends linearly on θ , it was possible to use available data to calculate the lift for any given value of θ , as a function of the U and α_s values measured. Using this method it was also possible to extrapolate to values of θ lower than those measured (i.e. lower than 2 to 4deg). The value of θ corresponding to MPOG was unknown at the time, but assuming $\theta=1$ deg seemed to provide the best fit to the values of lift previously measured with an S-76 during the Foinaven FPSO trials.

The variation of lift with U and α_s (extrapolated to $\theta=1$ deg) is shown in Figure 3 (datapoints shown as squares). From Figure 3 it is clear that the variation of lift with wind speed is linear at first, but tails off at higher wind speeds. The slope of the variation depends on α_s . A simple empirical fit to this variation was derived as follows (plotted as lines in Figure 3):

$$(6) \quad R(U, \alpha_s) = \begin{cases} (L_U + L_\alpha \cdot \alpha_s) \cdot U + R_0 & \text{if } 0 \leq U \leq U_L \\ L_\alpha \cdot \alpha_s \cdot U + R_1 & \text{if } U > U_L \end{cases}$$

L_U , L_α , R_0 and R_1 are empirical constants which depend on the value of θ , and U_L is equal to:

$$(7) \quad U_L = \frac{R_1 - R_0}{L_U}$$

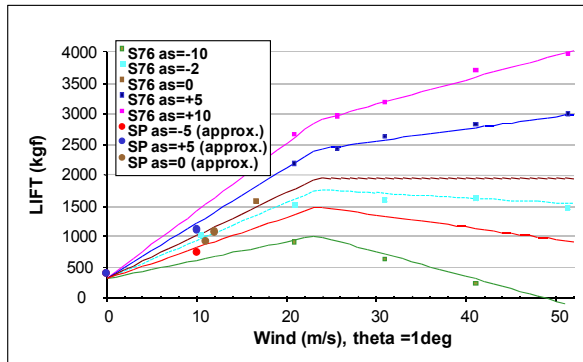


Figure 3: The variation of main rotor lift as a function of wind speed U and angle of attack, α_s , for $\theta=1$ deg.

Measurements from the Super Puma trials in Aberdeen are plotted on the same graph (circles), to allow a direct comparison with S-76 data. Not only is the variation of the lift with wind speed similar to the NASA Ames data, but also the variation with α_s .

It is not clear why the S-76 and the Super Puma should produce similar amounts of lift at MPOG despite the large difference in rotor size. Anecdotal evidence from pilots suggests that the S-76 produces a lot more downwash than other helicopter types of similar size at MPOG, and thus more lift for its size of rotor. It is not possible to generalise the empirical expression for the lift given in (6) above to other helicopter types; the lift would have to be measured directly.

Another way of estimating the lift at MPOG has been proposed and tested. Assuming that the lift varies linearly with θ , it is possible to estimate the value of lift at MPOG if the values of θ at MPOG and in the hover are known. In the hover the lift is simply equal to the weight of the helicopter; noting the corresponding value of θ , and repeating this for a few different helicopter weights, will provide a linear correlation for θ , at a given wind speed. The lift at MPOG can be extrapolated from these values based on the θ value at MPOG.

Such hover data for the S-76 (gathered as part of a trial unrelated to this project) were measured and provided courtesy of FRASCA [4]. It was confirmed that at MPOG, $\theta=4$ deg for the S-76. The lift values calculated from the data in [4], matched those measured onboard the Foinaven and the NASA Ames values corresponding to $\theta=1$ deg. It is not understood, however, why there should be an offset between the collective pitch values in the NASA Ames dataset (which were obtained with an actual, full size S-76 rotor) and those measured on aircraft; nonetheless, all measured and inferred values of S-76 lift are consistent.

2.5 Main rotor torque

The torque acts on the helicopter fuselage in a direction opposite to the direction of rotation of the main rotor. It also acts in the plane of the main rotor disc (i.e. inclined relative to the helideck by an angle γ). It is assumed that no other (flapping) moments are transmitted to the helicopter fuselage since the blades are freely hinged.

The torque is assumed constant with wind speed, as a first approximation (this assumption is also supported by the NASA Ames dataset). The actual value of the main rotor torque is not provided in flight manuals nor recorded (only the relative % torque settings), and therefore this had to be estimated based on other limited data available. However, helicopter OEMs are expected to have access to this data.

2.6 Control forces – cyclic and pedal

Cyclic and pedal control forces are used in flight to oppose the main rotor torque and to manoeuvre the helicopter. When on deck, the cyclic and pedal controls are set to their central settings, with the assumption that this does not generate any additional sideways forces/moments on the helicopter. The Aberdeen Super Puma trials data indicated that, at MPOG with control settings set to central, control forces were indeed nearly equal to zero.

In addition, controls were exercised either side of central during the Foinaven S-76 trials as well as the Aberdeen Super Puma trials, to assess their effect on stability. Differences in the reaction forces at each helicopter wheel were used to infer the control forces acting on the helicopter. With this approach it is not possible to differentiate between forces and pure moments generated by the rotor; the total moment generated by exercising the controls was calculated and expressed as equivalent F_{CX} and F_{CY} forces acting at the main rotor hub. These were found to vary linearly with control setting.

By contrast to the main rotor lift, the data from the trials did not indicate a significant variation of these control forces due to wind speed; however it is noted that the control forces could not be measured as accurately as the lift.

2.7 Measuring the vertical CoG position (CGZ)

As discussed in more detail in the sections that follow, modelling the on-deck stability of a helicopter requires accurate information on the location of the CoG and the mass of the helicopter.

The mass (m), and longitudinal and lateral positions of the CoG (CGX and CGY , respectively) is carefully calculated in advance of each helicopter operation to ensure compliance with flight manual limits. This

calculation is based on regular ‘scheduled weighs’ of m , CGX and CGY of each helicopter when empty, subsequently adding the effect of each and every additional item (passengers, cargo or fuel) for each given flight.

However, there is no requirement to calculate the vertical position of the CoG (CGZ), and this information was unknown to helicopter operators in the North Sea at the early stages of this project. Helicopter OEMs have this information, since they are able to calculate the CGZ by adding together the moment arms of each of the components of the helicopter. This information is typically kept confidential.

Not having access to this information, an alternative method was devised during the Aberdeen Super Puma trials in order to calculate CGZ directly. The solution was to adapt the procedure already used during the scheduled weighs. The helicopter is lifted by three weighing jacks and great care is taken to ensure that the helicopter is perfectly level; the loads measured at each of the jacking points are then used to calculate CGX and CGY very accurately. By intentionally misaligning the helicopter slightly in roll (by about 1-2deg, taking care to measure this angle accurately), it is then possible to infer CGZ very accurately.

During the Aberdeen Super Puma trials, CGZ measurements were made for a helicopter low in fuel and with a helicopter with full tanks. Values later provided by the helicopter OEM matched the measured values very closely.

2.8 Undercarriage deflection

Undercarriage deflections are expected to affect helicopter stability in three main ways (as illustrated in Figure 4):

- by shifting the location of the centre of gravity and the points of action of all other forces;
- by altering the components of forces that are fixed to the helicopter; e.g. creating a sideways component of main rotor lift (the components of the gravitational/inertial forces relative to the helideck are unaffected);
- by altering the helicopter incidence to the wind; this can affect main rotor lift by changing the rotor disc angle of attack, α_s ; the effect on fuselage drag is expected to be negligible.

It is possible to model all the above effects if the inclination of the helicopter relative to the helideck is known. However, quantifying this inclination presents some considerable difficulties since it can arise either:

- due to the ‘twist’ generated in the undercarriage as a result of landing with the brakes applied (helicopters land with one main wheel lower than the other as a result of the control forces needed to counteract the main rotor torque in the hover prior to landing), or
- in response to the forces acting on the helicopter, making the oleo deformation and the forces implicitly related. The deflection response of the undercarriage is complex and non-linear; such information is typically proprietary to helicopter OEMs. Also, the undercarriage will respond dynamically to the transient forces acting on the helicopter; a simple quasi-static approach to modelling the forces acting on the helicopter could lead to an underestimate of resonance effects, or an overestimation of forces by not accounting for inertial and/or damping effects.

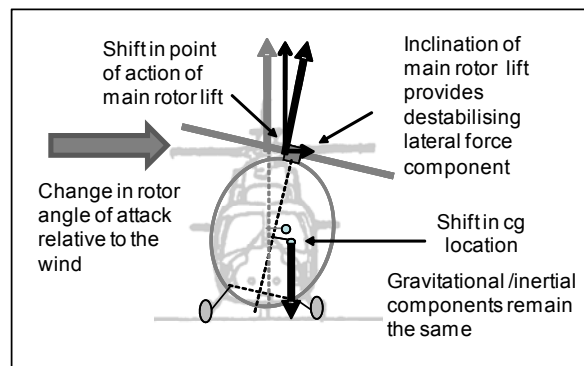


Figure 4: Destabilising effect of helicopter inclination relative to the helideck due to uneven oleo deflection.

3. LOSS OF ON-DECK STABILITY

Loss of equilibrium occurs when the total moment of the ‘external’ forces listed above can no longer be balanced by the moments of the helideck reaction forces acting normal to the helideck, and of the frictional forces acting in the plane of the helideck to resist motion. There are two main modes of failure: tipping and sliding.

It is noted that only helicopters with a nose wheel tricycle undercarriage are considered in the analysis that follows, since this represents the type most used in the North Sea.

For tipping failure, a rotation about the axis connecting the nose wheel (N) and any of the main wheels (Starboardside (S) or Portside (P)) has to occur (tipping axes NP or NS).

Sliding can occur in translation or in rotation. A rotational slide is more likely since only two of the

wheels have to move instead of all three. Which two wheels will slide first will depend on the balance of moments, and thus each sliding scenario (about N, P or S) has to be considered in turn.

4. DEFINING THE RESERVE OF ON-DECK STABILITY

Having identified each mode of failure, the reserve of on-deck stability (ROS) for each mode can be defined by considering the balance of moments about the rotation axis for each failure mode. For tipping failure this is the NS or NP axis, and for rotational slide modes, it is a rotation relative to the axis normal to the helideck.

Considering the ratio of destabilising versus restoring moments, the ROS has been defined as follows:

$$(8) \text{ Reserve of Stability} = 1 - \left| \frac{\text{destabilising moments}}{\text{restoring moments}} \right|$$

This is equal to zero at the point of failure and equal to 1 (100%) when no destabilising forces act on the helicopter.

For tipping failure, the destabilising moments are assumed equal to the total moment of the gravitational and inertial forces acting sideways on the helicopter (i.e. in the plane of the helideck) plus that of all other external forces. The gravitational and inertial forces acting normal to the helideck always act to restore equilibrium and thus the denominator is assumed equal to the moment of these forces. This restoring moment is effectively constant and does not depend on any of the other external forces.

For sliding failure, the only forces consistently acting to restore equilibrium are the frictional forces. The restoring moment is therefore that of the frictional forces, relative to an axis normal to the helideck. All other external forces generate the total destabilising moment.

To maintain equilibrium, the frictional restoring moment will adapt to always balance the destabilising moment of the external forces. In order to have a meaningful definition for the reserve of stability, the maximum value of the frictional restoring moment is used in the denominator. This is simply the moment due to each of the frictional forces assuming the maximum value of $\mu \cdot F_R$, where μ is the helideck coefficient of friction and F_R is the reaction force on each wheel. However, the reaction force on each wheel does depend on all other forces acting on the helicopter.

5. ANALYTICAL EXPRESSIONS FOR THE RESERVE OF STABILITY

Using the definition in (8) the reserve of stability can be calculated by modelling all the forces/moments acting on a helicopter, e.g. with a helicopter numerical model such as FlightLab.

However, understanding the effect of helideck motion presents a challenge, since several input parameters are needed to describe the helideck motion fully: roll, pitch, and helideck accelerations in three directions. In order to set practical operational limits, the effect of all helideck motion parameters had to be consolidated into a single helideck motion parameter, the Measure of helideck Motion Severity (MMS).

A numerical helicopter model provides limited insight in this respect, hence an analytical approach was applied to the calculation of the Reserve of Stability. As discussed below, this has provided much insight into the destabilising effect of helideck motion, as well as the relative contribution of all other destabilising forces, for all modes of failure (tipping and sliding).

This analysis has also underpinned the derivation of operational limits curves, as discussed later in Section 6.

5.1 Tipping failure (NS, NP axes only)

Tipping can occur relative to axes NS, NP or with the lifting of the Nose wheel relative to axis PS. The latter tipping mode is unlikely, however, and the expressions derived for this mode of failure will not be included in the discussion that follows.

NS and NP tipping modes are symmetrical relative to the longitudinal (x-axis) of the helicopter. The calculation presented here is for the NS failure mode, but it can easily be adapted for the NP axis.

5.1.1 Destabilising effect of helideck motion only

Consider first a helicopter on a moving helideck with no other forces acting on it other than gravitational and inertial forces. The total external force acting on the helicopter is then equal to $m \cdot \vec{a}$, where \vec{a} is the total acceleration of the helideck (gravitational and inertial).

This force can be resolved normal to the helideck and parallel to the helideck. The component acting normal to the helideck, $m \cdot a_z$, provides a restoring moment, and the component parallel to the helideck, $m \cdot a_n$, provides a destabilising moment.

Figure 5 defines the right handed coordinate system used throughout, defined with the z axis pointing downwards, and normal to the helideck. The x- and

y-directions are defined relative to the three helicopter contact points (y-axis parallel to PS).

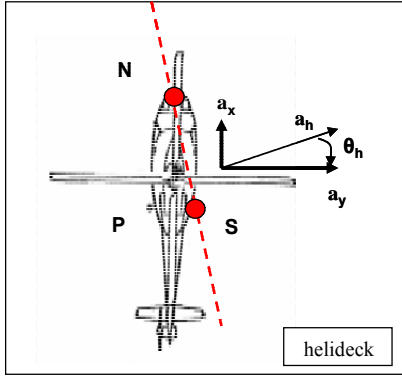


Figure 5: Definition of the orientation factor angle θ_h , and resultant horizontal acceleration, a_h .

As shown in Figure 5, a_h is the resultant of the helideck acceleration components a_x and a_y . The angle of a_h relative to the lateral axis of the helicopter is the “orientation angle”, θ_h , defined as:

$$(9) \quad \tan \theta_h = \frac{a_x}{a_y}$$

The reserve of stability (ROS) due to the effect of helideck motion only is equal to:

$$(10) \quad ROS_{TIP} = 1 - \frac{\text{destabilising moment of } m \cdot a_h}{\text{restoring moment of } m \cdot a_z}$$

It can be shown that this is equal to:

$$(11) \quad 1 - \left(\frac{FR}{L} \cdot \cos \theta_h + \frac{LY}{L} \cdot \sin \theta_h \right) \cdot \frac{a_h}{a_z} \cdot \frac{CGZ}{CGX \cdot \frac{LY}{L} - CGY \cdot \frac{FR}{L}}$$

where CGX is the longitudinal distance of the CoG from the nose wheel of the helicopter, CGY is the lateral offset of the CoG relative to the helicopter centreline, CGZ is the height of the centre of gravity above the helideck. FR is the distance between the nose and main wheels, LY is half the distance between the main wheels, and L is the distance between the nose wheel contact point, and that of any of the two main wheels.

Thus, the destabilising effect of the helideck motion depends on: a) the ratio of a_h/a_z , b) the “orientation angle”, θ_h , c) the location of the CoG and d) the dimensions of the helicopter’s undercarriage. As discussed further in [1], the ratio a_h/a_z was identified as the single most representative “Measure of Helideck Motion Severity” (MMS). The “orientation angle”, θ_h will depend on the orientation of the helicopter relative to the helideck at the time of landing, and will subsequently change continuously with the motion of the helideck.

The factor:

$$(12) \quad O_{FTIP} = \frac{FR}{L} \cdot \cos \theta_h + \frac{LY}{L} \cdot \sin \theta_h$$

has been termed the ‘orientation factor’.

It multiplies the destabilising effect of the MMS and represents the effect of helicopter orientation on the helideck. O_f is maximum when a_h is oriented normal to the (NS or NP) tipping axes of the helicopter and zero when a_h is parallel to either of the tipping axes NP or NS. Its maximum value is equal to:

$$(13) \quad O_{FTIPmax} = \sqrt{\left(\frac{FR}{L}\right)^2 + \left(\frac{LY}{L}\right)^2} = 1$$

Therefore, the ROS of a helicopter can be quantified simply as:

$$(14) \quad ROS_{TIP} = 1 - MMS \cdot O_{FTIP}(\theta_h) \cdot f_{grav}$$

where f_{grav} is a purely geometrical term, equal to:

$$(15) \quad f_{grav} = \frac{1}{\frac{CGX}{CGZ} \cdot \frac{LY}{L} - \frac{CGY}{CGZ} \cdot \frac{FR}{L}}$$

The above factor was derived for failure about axis NS; the same result applies to the NP tipping mode but using the opposite sign for the CGY term, and the opposite sign for the angle θ_h in O_{FTIP} .

5.1.2 Destabilising effect of all other forces

Considering the effect of all other forces, \vec{F} , and pure moments, \vec{M} , it can be shown that ROS_{TIP} can be expressed in the simple form:

$$(16) \quad 1 - MMS \cdot O_{FTIP}(\theta_h) \cdot f_{grav} - \sum \left(\frac{\vec{F} \cdot \vec{f}_{ROS}}{m \cdot a_z} \right) - \sum \left(\frac{\vec{M} \cdot \vec{f}_{mROS}}{m \cdot a_z} \right)$$

where:

$$f_{ROS} = \begin{pmatrix} CFZ \cdot \frac{LY}{L} \\ CFZ \cdot \frac{FR}{L} \\ \frac{FR}{L} \cdot CFY - \frac{LY}{L} \cdot CFX \end{pmatrix} \quad f_{mROS} = \begin{pmatrix} \frac{FR}{L} \\ -\frac{LY}{L} \\ 0 \end{pmatrix}$$

are matrices containing purely geometrical factors reflecting the undercarriage geometry (as defined previously) and the point of action of each force; at any arbitrary location CFX (longitudinal distance from front wheel), CFY (lateral offset relative to centreline), and CFZ (height above the helideck).

The maximum ROS is equal to 1; this decreases as a result of the destabilising forces/moments acting on the helicopter, as indicated by the minus sign in front of each of the terms.

Depending on the orientation of the forces relative to failure axis, some forces/moments can have a stabilising effect, reflected by a positive term in the equation above, leading to an increase of ROS. The ROS can in fact become greater than 1, when forces act in a stabilising direction.

Values for f_{ROS} and m_{ROS} presented above are for the NS tipping mode; values for the NP tipping mode have also been derived by considering the symmetry relative to the x-axis.

5.1.3 Calculating the ROS from vertical reaction forces

It can be shown that, in general, there is a direct, proportional relationship between the reserve of stability and the helideck reaction forces.

In the case of tipping failure, helideck reaction forces act normal to the helideck to balance the total weight of the helicopter ($m \cdot a_z$). Helideck reaction forces are distributed between the wheels in such a way as to exactly counterbalance the net restoring moment acting on the helicopter as a result of all the other 'external' forces acting on the helicopter.

Thus, measuring the reaction forces provides a direct way of calculating the reserve of stability, and it can be shown that the reserve of stability for tipping failure, for each of the tipping axes, is equal to:

$$(17) \quad ROS_{TIP_NS} = \frac{2 \cdot FR \cdot LY}{LY \cdot CGX_f + FR \cdot CGY} \cdot \frac{F_{RS}}{m \cdot a_z}$$

$$ROS_{TIP_NP} = \frac{2 \cdot FR \cdot LY}{LY \cdot CGX_f - FR \cdot CGY} \cdot \frac{F_{RP}}{m \cdot a_z}$$

where F_{RS} , F_{RP} , are the normal reaction forces at the two main wheels (Port and Starboard), and CGY is assumed positive when offset towards starboard. Due to symmetry, the only difference in the expressions for NS and NP is in the sign of CGY .

The reserve of stability for sliding failure can, in principle, also be calculated based on measurements of the reaction forces, provided that the helideck coefficient of friction, μ , is known.

It is possible to measure the helideck reaction forces normal to the helideck by placing the wheels of a helicopter on load cells. This method has been used

successfully during helicopter trials offshore on the Foinaven FPSO and on the ground at Aberdeen airport. In theory, it would be also possible to measure the reaction forces in the plane of the helideck using a three-component load cell; however, this approach has not yet been attempted in practice.

It is also possible to measure the normal reaction forces by adding instrumentation directly to the helicopter undercarriage (e.g. using strain gauges). This is a promising idea, since it would allow the reserve of stability to be measured in real time on an instrumented helicopter, providing an alarm to pilots if ROS_{TIP} and/or ROS_{SLIDE} were to drop to a dangerously low level. However, this is of limited operational use, since pilots need to establish whether on-deck conditions will be safe prior to landing.

5.2 Sliding failure

In the case of tipping failure, because the restoring moment in the denominator of the ROS is effectively constant, the ROS can be expressed in the simple form shown in (16), which breaks into a number of separate terms representing the destabilising contribution of each individual force or moment.

However, because the restoring moment of the frictional forces is implicitly related to the destabilising moments, the ROS expression for sliding results in a complex ratio, with gravitational and other force terms appearing in both the numerator and denominator.

Thus, in contrast to the expression derived for tipping, the analytical sliding expressions for the ROS for sliding are not very physically intuitive. Nonetheless, these expressions have allowed limits curves for sliding to be derived, as discussed in Section 6.2.

6. ANALYTICAL LIMITS CURVE EXPRESSIONS

6.1 Tipping failure

Since failure occurs when the ROS falls to zero, the 'critical' value of MMS_{crit} above which failure will occur can be calculated by setting the ROS expressions to zero, and solving for MMS .

Applying this to equation (16), it follows that the MMS_{crit} for tipping can be expressed as:

$$(18) \quad \left(1 - \sum \frac{\vec{F} \cdot f_{ROS}}{m \cdot a_z} - \sum \frac{\vec{M} \cdot m_{ROS}}{m \cdot a_z} \right) \cdot \frac{1}{O_{FTIP}(\theta_h) \cdot f_{grav}}$$

where f_{grav} , f_{ROS} , fm_{ROS} , and O_{TIP} are as previously defined. The expression for MMS_{crit} can also be recast as:

$$(19) \quad MMS_{maxTIP} = \frac{1}{O_{fTIP}} \cdot \sum \frac{\vec{F} \cdot f}{m \cdot a_z} - \frac{1}{O_{fTIP}} \cdot \sum \frac{\vec{M} \cdot fm}{m \cdot a_z}$$

where:

$$f = f_{ROS}/f_{grav}, \quad fm = fm_{ROS}/f_{grav}$$

and MMS_{maxTIP} , is equal to:

$$(20) \quad \frac{1}{O_{fTIP} \cdot f_{grav}} = \frac{1}{O_{fTIP}} \left(\frac{CGX \cdot LY}{CGZ \cdot L} - \frac{CGY \cdot FR}{CGZ \cdot L} \right)$$

MMS_{maxTIP} is the maximum possible value of MMS_{crit} , which applies when no destabilising forces other than gravitational/inertial act to reduce the ROS. Any force/moment in a destabilising direction will reduce the value of MMS_{crit} , as represented by the minus sign in each of the other force/moment terms.

The lift ($R(U, \alpha_s)$) and fuselage drag force ($k_w \cdot U^2$) terms in the $MMS_{critTIP}$ equation are as follows:

Main rotor lift:

$$(21) \quad \frac{1}{O_{fTIP}} \cdot \left(\frac{HMR}{CGZ} \cdot |\sin \gamma| + \frac{FA}{CGZ} \cdot \cos \gamma \right) \cdot \frac{LY}{L} \cdot \frac{R(U, \alpha_s)}{m \cdot a_z}$$

Fuselage drag:

$$(22) \quad \frac{1}{O_{fTIP}} \cdot \left(k_{wx} \cdot \frac{CPZ \cdot LY}{CGZ \cdot L} + k_{wy} \cdot \frac{CPZ \cdot FR}{CGZ \cdot L} \right) \cdot \frac{U^2}{m \cdot a_z}$$

where FA is the distance of the main rotor from the Nose wheel, HMR the height of the rotor hub above ground. and CPX, CPZ are the corresponding distances for the Centre of Pressure. The coefficients k_{wx} and k_{wy} correspond to wind drag force components in x and y.

The above two terms are a function of U, the lift force term is linear and the drag term is quadratic. Other forces acting on the helicopter (e.g. main rotor torque, control forces) may also be dependent on the wind, but available evidence suggests that this dependence is significantly less strong than that of the lift and drag.

Therefore Equation (16) provides an expression for MMS_{crit} as a function of wind speed U. This defines the shape of the operational limits curve (as described in more detail in [1]).

For tipping, it is also possible to calculate the limiting curve for any required threshold of stability (i.e. introducing an added safety margin of $M\%$, say). It can be shown that this is the same as equation (19), but with the MMS_{maxTIP} term multiplied by $(1-M\%)$.

6.2 Sliding failure

Although the ROS equations were quite complex, the MMS_{crit} expressions for sliding can be cast into a simple form, identical to that of the tipping modes:

$$(23) \quad MMS_{crit} = MMS_{max} - \frac{1}{O_f} \cdot \sum \frac{\vec{F} \cdot f}{m \cdot a_z} - \frac{1}{O_f} \cdot \sum \frac{\vec{M} \cdot fm}{m \cdot a_z}$$

but with different geometric factors f, fm, and O_f , which also include the coefficient of helideck friction, μ .

These factors are different for each of the sliding failure modes (about the Nose wheel, and about any of the main wheels(S or P)). The failure mode that will occur first will be that with the lowest MMS_{crit} .

6.2.1 Sliding about nose wheel (N)

The terms of the MMS_{crit} equation (23) for sliding about the nose wheel (N) are:

$$(24) \quad MMS_{max} = \frac{1}{O_{fN}} \cdot \left(\frac{CGX}{CGZ} \cdot \mu \right)$$

where O_{fN} is an orientation factor equal to:

$$O_{fN} = \frac{CGX}{CGZ} \cdot \frac{FR}{L} \cdot \cos \theta_h + \left(\mu + \frac{CGY}{CGZ} \cdot \frac{FR}{L} \right) \cdot \sin \theta_h$$

The geometrical matrix factors are:

$$(25) \quad f = \begin{pmatrix} \mu \cdot \frac{CFZ}{CGZ} + \frac{CFY}{CGZ} \cdot \frac{FR}{L} \\ \frac{CFX}{CGZ} \cdot \frac{FR}{L} \\ -\mu \cdot \frac{CFX}{CGZ} \end{pmatrix} \quad fm = \begin{pmatrix} 0 \\ -\mu \cdot \frac{1}{CGZ} \\ \frac{FR}{L} \cdot \frac{1}{CGZ} \end{pmatrix}$$

This is for an anticlockwise rotation, consistent with forces causing tipping relative to NS.

6.2.2 Sliding about main wheel S

To include the special case that the nose wheel is free to castor, the coefficient of friction at the nose wheel has been assumed equal to $\alpha \cdot \mu$, i.e. a fraction α of the coefficient at the two other wheels. When the wheel is unlocked and free to castor $\alpha=0$, otherwise, if locked, it is assumed that $\alpha=1$.

The terms of the MMS_{crit} equation (23) for sliding about the nose wheel (S) are:

$$(26) \quad MMS_{max} = \frac{1}{O_{fS}} \cdot \left[\left(\alpha \cdot \frac{FR - CGX}{CGZ} + \frac{LY}{L} \cdot \frac{CGX}{CGZ} \right) - \frac{FR}{L} \cdot \frac{CGY}{CGZ} \right] \cdot \mu$$

where O_{fS} is an orientation factor equal to:

$$\frac{FR}{L} \left(\frac{FR - CGX}{CGZ} + \mu \right) \cdot \cos \theta_h + \left[\frac{FR}{L} \cdot \frac{(LY - CGY)}{CGZ} - \mu \cdot \left(\alpha - \frac{LY}{L} \right) \right] \cdot \sin \theta_h$$

The geometrical matrix factors for a clockwise rotation (consistent with forces causing tipping relative to NS), are:

$$(27) \quad f = \begin{bmatrix} \frac{FR}{L} \cdot \frac{(LY - CFY)}{CGZ} - \mu \cdot \left(\alpha - \frac{LY}{L} \right) \cdot \frac{CFZ}{CGZ} \\ \frac{FR}{L} \cdot \left[\frac{(FR - CFX)}{CGZ} + \mu \cdot \frac{CFZ}{CGZ} \right] \\ -\mu \cdot \left[\alpha \cdot \frac{(FR - CFX)}{CGZ} + \frac{LY}{L} \cdot \frac{CFX}{CGZ} \right] + \mu \cdot \frac{CFY}{CGZ} \cdot \frac{FR}{L} \end{bmatrix}$$

$$f_{im} = \begin{bmatrix} \mu \cdot \frac{FR}{L} \cdot \frac{1}{CGZ} \\ \left(\alpha - \frac{LY}{L} \right) \cdot \mu \cdot \frac{1}{CGZ} \\ \frac{FR}{L} \cdot \frac{1}{CGZ} \end{bmatrix}$$

7. EXAMPLES OF IN-SERVICE ROS CALCULATIONS

The ROS and limits curves have been expressed as a function of the main forces acting on the helicopter. These analytical results are exact, but modelling the individual forces acting on the helicopter is subject to a number of assumptions and uncertainties, as discussed previously in Section 2.

There are two main sources of available data: that allow in-service ROS values to be calculated:

- Data from S-76 field trials onboard FPSO Foinaven (carried out in 1999).
- Data from the investigation of the G-BKZE Super Puma accident onboard the drillship West Navion (in November 2001).

It is only possible to provide a very high-level summary of the main results and conclusions drawn from the analysis of this data. More detail will be included in the final report [5].

7.1 Analysis of Foinaven trials data

7.1.1 Introduction

Atkins had subcontracted DERA (the Defence and Evaluation Research Agency UK) to carry out field trials onboard the FPSO Foinaven in November 1999, using an S-76 helicopter, operated by Bond Helicopters.

The aim of the trials was to provide data to validate the helicopter stability model. Four tests were carried out: two with rotors stationary and two with rotors running at MPOG, with the helicopter oriented

aligned with the vessel's longitudinal axis and one at right angles to it (as illustrated in Figure 6).

Load cells were positioned under each of the wheels of the helicopter, the motion of the helideck was monitored using MRUs (Motion Reference Units), and the wind was measured with an ultrasonic anemometer at the edge of the helideck.

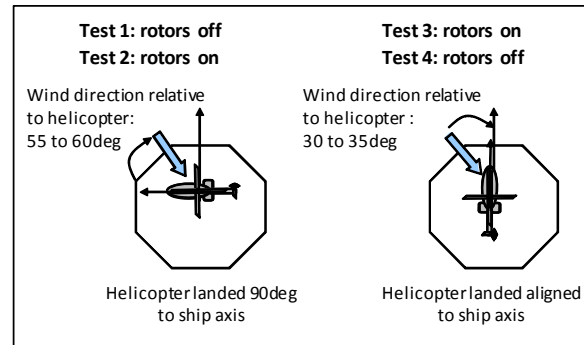


Figure 6: S-76 trials onboard Foinaven: illustration of helicopter orientation and relative wind direction for each of the four tests.

7.1.2 Evaluating the main rotor lift model

Summing the vertical reactions at each wheel and subtracting the gravitational and inertial forces (calculated using the information from the MRUs and by fine-tuning estimates of the helicopter mass using rotors-off measurements), it was possible to calculate the main rotor lift at MPOG accurately (Figure 7).

Modelling the main rotor lift using the expression in Equation (7) requires two main parameters, wind speed U and rotor disc angle of attack, α_s . Measuring U is straightforward; α_s can be calculated using the wind velocity components in the plane of the helideck and normal to the helideck, the tilt of the main rotor γ , and the orientation of the helicopter relative to the wind. However, this is relatively complex to do.

Although the value of U measured during the trials is considered robust, the value of α_s that can be inferred from the trials measurements is uncertain. The anemometer readings indicated an updraft at the helideck that was very large (5m/s in a 12m/s wind, far larger than the vertical wind component limit of ± 0.9 m/s that used to be recommended in CAP437). This could be the effect of localised flow deflection at the edge of the helideck, where the anemometer was mounted.

As a result it is not possible to evaluate Equation (7) fully based on the Foinaven trial information. What can be inferred however, is the mean value of α_s that would lead to values of lift closest to those measured. This is illustrated in Figure 8, which

shows the sensitivity of the modelled lift to wind speed and α_s .

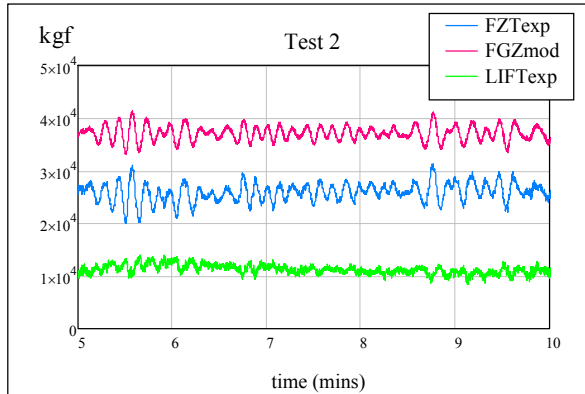


Figure 7: The lift force is calculated by taking the difference between the sum of the vertical reactions (FZT_{exp}) and the modelled gravitational and inertial component normal to the helideck (FGZ_{mod}).

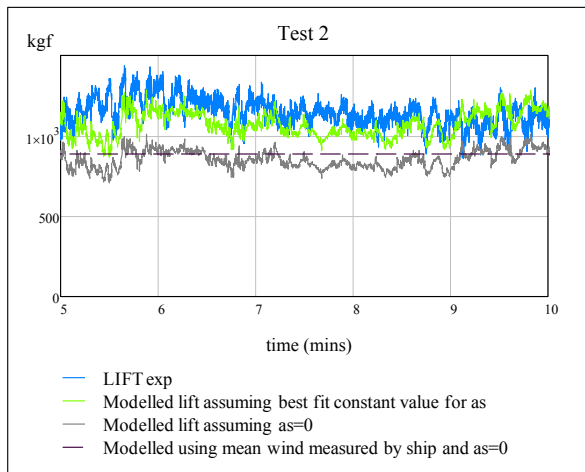


Figure 8: Modelling the lift using various assumptions for the value of α_s .

7.1.3 Modelling other forces

From the difference between the main wheel load cell measurements, the total lateral force acting on the helicopter (referred relative to the CoG) could be inferred. However, this depends on the accuracy with which the CoG and helicopter mass can be estimated (and which change during rotors running trials, due to the fuel burn).

For rotors off tests, the agreement between the force inferred from the load cell measurements ('exp') and a quasi-static calculation of the gravitational/inertial and fuselage drag forces ('mod') was reasonable, as illustrated by the example shown in Figure 9.

By contrast, the total lateral force acting on the helicopter for rotors running tests was significantly higher than that during the rotors off tests (as

illustrated in Figure 10), and higher than the value from the quasi-static calculation ('mod'). This included the gravitational/inertial forces, fuselage drag, and main rotor torque. The lift was assumed to act vertically upwards, thus generating no lateral component.

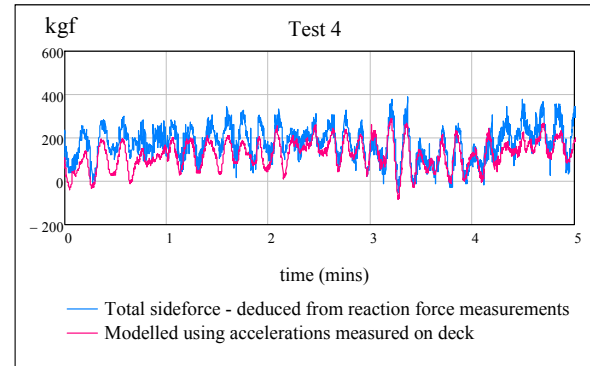


Figure 9: Test with rotors off - comparison of total sideforce.

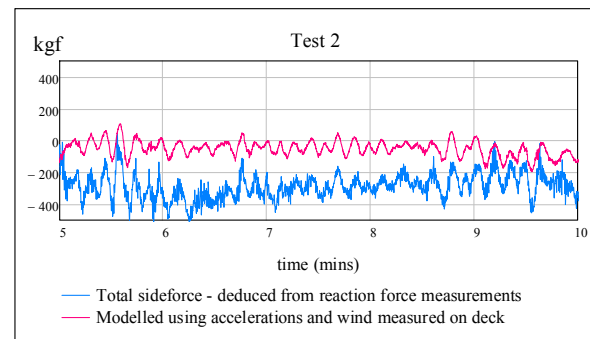


Figure 10: Difference in lateral force between that modelled and measured, and comparison with lift force measured.

There are a number of possible explanations:

- Control forces were assumed equal to zero; FDR data of control settings during the trials were not kept, so it is not known with certainty if the controls were indeed central during the trials.
- Even if cyclic and/or pedal controls were correctly centred, it is still possible that an additional force/moment could have been generated due to the interaction of the wind with the main rotor.
- A helicopter roll inclination relative to the helideck (e.g. due to uneven oleo deflection) could create a significant lateral component of main rotor lift, as well as increase the gravitational lateral component. Oleo deflection effects were not modelled in this example, but the helicopter was indeed inclined relative to the helideck during the tests by varying amounts in each test, up to 2deg on average.

7.1.4 Modelling the ROS (tipping failure only)

The reserve of stability (ROS) for both tipping axes (NP and NS) was calculated in two ways:

- 'R_{TIPexp}': directly from load cell measurements, using equation (17).
- 'R_{TIPmod}': using the quasi-static calculation described previously. The lift force was modelled using a constant value for α_s (giving the closest agreement with the measured lift, as previously discussed).

The results are compared in Figure 11 below (only a subset of the time series modelled is shown for clarity).

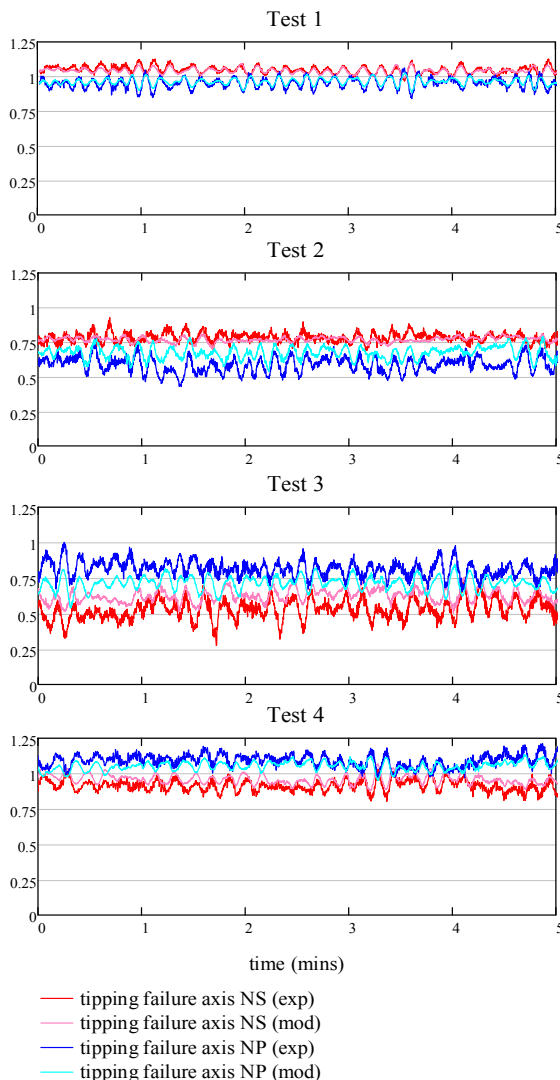


Figure 11: Comparison of the reserve of stability relative to the two roll-over axes.

When rotors are stationary, the experimentally derived values R_{TIPexp} show that there is a modest reduction in the reserve of stability. Comparing the

modelled values to those derived experimentally, the agreement in Test 1 is very close, and the agreement in Test 4 is also good (the mean differs only by 5% and the max by 10%); this is consistent with the good agreement between the modelled and experimentally derived lateral forces. When rotors are turning, there is a marked reduction in the experimentally derived ROS, down to a minimum of about 25%, compared to 75% when rotors were stationary. However, the modelled values underestimate this reduction by a significant margin (the worst case minimum value is 42% instead of 25%). Since the lift was adjusted in this example to fit the experimental data, the difference between R_{TIPexp} and R_{TIPmod} reflects the effect of a significant rotor-induced lateral force, which as previously discussed, is not fully accounted for.

7.2 G-BKZE accident investigation

A tipping failure accident involving an AS332 L2 Super Puma (G-BKZE) occurred on the helideck of the West Navion drillship following a successful landing, disembarkation of passengers, and refuelling.



Figure 12: Super Puma G-BKZE accident onboard the West Navion drillship, November 2001.

The helideck was within pitch, roll and heave limits, and the mean wind speed was 32kts. Owing to a failure in the ship's dynamic positioning (DP) system, the heading of the vessel started drifting about 7 minutes after touchdown. After a further 5.5 minutes the aircraft tipped over, coming to rest on its side, causing significant damage to the aircraft, seriously injuring the co-pilot who was on the helideck outside the aircraft at the time, and damage to the surface of the helideck (Figure 12).

Several agencies had attempted to model the forces and moments acting on the helicopter when the accident occurred, and all were unable to explain why the helicopter had rolled over.

The Air Accidents Investigation Branch (AAIB) contracted Atkins to assist the investigation, using the numerical helicopter stability model that was being developed at the time. The model was used to establish whether helicopter tipping and/or sliding failure would have been expected given the available information from the accident.

The results from the stability model were consistent with what had occurred, and provided a clear and credible explanation of the accident [6]. The most crucial elements in this explanation were the assumption for the main rotor lift (consistent with Equation (6)), and taking into account the effect not only of the mean wind speed but also that of gusts.

Simulated trends for the ROS shown in Figure 13 were consistent with the time and mode of failure (sliding occurring slightly ahead of tipping failure).

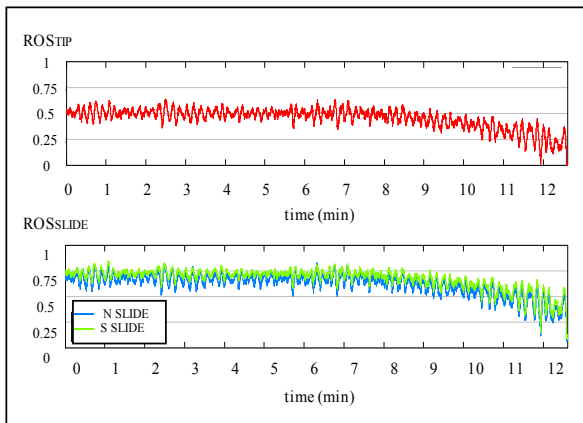


Figure 13: Modelled ROS_{TIP} (upper plot) and ROS_{SLIDE} for both sliding failure modes (lower plot), leading up to the time of the G-BKZE accident.

8. CONCLUSIONS AND RECOMMENDATIONS

A complete analytical model of helicopter stability has been developed that covers all modes of on-deck failure (tipping and sliding), for a nose wheel tricycle undercarriage helicopter.

Exact analytical expressions have been derived for the reserve of stability (ROS) and the limits curves, which are remarkably simple and physically intuitive. This has provided much insight on the destabilising effect of helideck motion, has underpinned the choice of MMS as an appropriate single measure of helideck motion severity, and has made the relative contribution of all other destabilising factors easy to understand and to assess.

Even though numerical helicopter stability models can be used to calculate the ROS, calculating limits curves without the insights presented in this paper would require a cumbersome iterative calculation to account for all possible combinations of helideck roll, pitch and accelerations.

The modelling framework presented in this paper for calculating the ROS and the limits curves provides an 'open source' platform for calculating operational limits curves, whatever the modelling approach used to calculate each of the forces or moments acting on the helicopter. This can also accommodate the effect of oleo deflection, by allowing changes to the components of forces and shifts in their points of action to be accounted for.

The analytical results presented in this paper are exact, but modelling the individual forces acting on the helicopter is subject to a number of assumptions and uncertainties.

It has been demonstrated how the main rotor lift at MPOG is a significant fraction of helicopter weight and is one of the main destabilising factors. An empirical model of main rotor lift has been presented, based on trials measurements and a meta-analysis of full-scale wind tunnel trials at NASA Ames. Remaining uncertainties in the modelling the main rotor lift and other associated lateral forces have also been discussed. A simple parametric representation to estimate the drag coefficient for any type of helicopter has also been described.

It is recommended that further work is carried out to improve the inputs and assumptions for modelling the forces and moments acting on the helicopter and, in particular, the modelling of the main rotor forces at MPOG.

Additional field measurements of the ROS, gathered in-service (e.g. using an instrumented undercarriage), would prove invaluable in this respect.

REFERENCES

- [1] A. Scaperdas, D. Howson "Developing New Operational Criteria for Landing and On-Deck Safety", **ERF 2012 Conference Proceedings, Paper 007**.
- [2] SF Hoerner "Fluid-dynamic drag: practical information on aerodynamic drag and hydrodynamic resistance" 1965 - Hoerner Fluid Dynamics.
- [3] Patrick M. Shinoda, "Full-Scale S-76 Rotor Performance and Loads at Low Speeds in the NASA Ames 80- by 120-Foot Wind Tunnel", Volume I, NASA Technical Memorandum 110379 USAATCOM Technical Report 96-A-004, April 1996
- [4] Personal communication – S-76 data provided by FRASCA, email of 20 October 2011.
- [5] Final Report "Defining safe operability limits for helicopters operating to moving offshore platforms", Atkins Report (in preparation, to be published as a CAA Paper).
- [6] "Investigation of the G-BKZE Super Puma incident", Atkins Report 5018762-R1, June 2003.